

# A COMPREHENSIVE REVIEW OF VERTICAL TAIL DESIGN

<b>Fabrizio Nicolosi</b> Associate Professor University of Naples “Federico II” – Dept. of Industrial Engineering (DII) Via Claudio 21, 80125, Naples – ITALY fabrnico@unina.it	<b>Danilo Ciliberti</b> Post-Doc University of Naples “Federico II” – Dept. of Industrial Engineering (DII) Via Claudio 21, 80125, Naples – ITALY danilo.ciliberti@unina.it	<b>Pierluigi Della Vecchia</b> Assistant Professor University of Naples “Federico II” – Dept. of Industrial Engineering (DII) Via Claudio 21, 80125, Naples – ITALY pierluigi.dellavecchia@unina.it
<b>Salvatore Corcione</b> Post-Doc University of Naples “Federico II” – Dept. of Industrial Engineering (DII) Via Claudio 21, 80125, Naples – ITALY salvatore.corcione@unina.it	<b>Vincenzo Cusati</b> Consultant University of Naples “Federico II” – Dept. of Industrial Engineering (DII) Via Claudio 21, 80125, Naples – ITALY vincenzo.cusati@gmail.com	

**Abstract.** This work deals with a comprehensive review of vertical tail design methods for aircraft directional stability and vertical tail sizing. The focus on aircraft directional stability is due to the significant discrepancies that classical semi-empirical methods, as USAF DATCOM and ESDU, provide for some configurations, since they are based on NACA wind tunnel tests about models not representative of an actual transport airplane. The authors performed RANS CFD simulations to calculate the aerodynamic interference among aircraft parts for hundreds configurations of a generic regional turboprop aircraft, providing useful results that have been collected in a new vertical tail preliminary design method, named VeDSC. Semi-empirical methods have been put in comparison on a regional turboprop aircraft, where the VeDSC method shows a strong agreement with numerical results. A wind tunnel investigation involving more than 180 configurations has validated the numerical approach. The investigation has covered both the linear and the non-linear range of the aerodynamic coefficients, including the mutual aerodynamic interference between the fuselage and the vertical stabilizer. Also, a preliminary investigation about rudder effectiveness, related to aircraft directional control, is presented. In the final part of the paper, critical issues in vertical tail design are reviewed, highlighting the significance of a good estimation of aircraft directional stability and control derivatives.

**Keywords.** Aircraft Design, Vertical tail, Stability and Control, CFD, Wind-Tunnel tests.

## 1 Introduction

The aircraft vertical tail is the aerodynamic surface that must provide sufficient directional equilibrium, stability, and control. Its sizing is determined by critical conditions as minimum control speed with one engine inoperative (for multi-engine airplanes) and landing in strong crosswinds.

The *airborne minimum control* speed  $V_{MC}$  is the calibrated airspeed at which, when the critical engine is suddenly made inoperative, it is possible to maintain control of the airplane with that engine still inoperative and maintain straight flight with an angle of bank of not more than  $5^\circ$  [1]. The airborne minimum control speed may not exceed 1.13 times the reference stall speed. Thus, it affects the takeoff field length, which must be kept as low as possible otherwise payload could be reduced when the aircraft is operating on short runways. The  $V_{MC}$  involves large rudder angles  $\delta_r$  to keep a small angle of sideslip  $\beta$ . See Figure 1 left. This requires a certain vertical tail area for a given rudder effectiveness  $\tau$ , which must be the highest possible to keep control authority at  $25^\circ$  or more of rudder deflection.

A *crosswind landing* requires a sufficient vertical tail area to ensure aircraft directional stability in this delicate phase, which involves large sideslip angles  $\beta$  in full flaps conditions and possibly large rudder angles  $\delta_r$  to keep the airplane at the desired flight path, although the rudder deflection is usually opposed to the sideslip angle, such that the vertical tail lift curve is in the linear range (like a plain flap at negative angle of attack, see Figure 1 right).

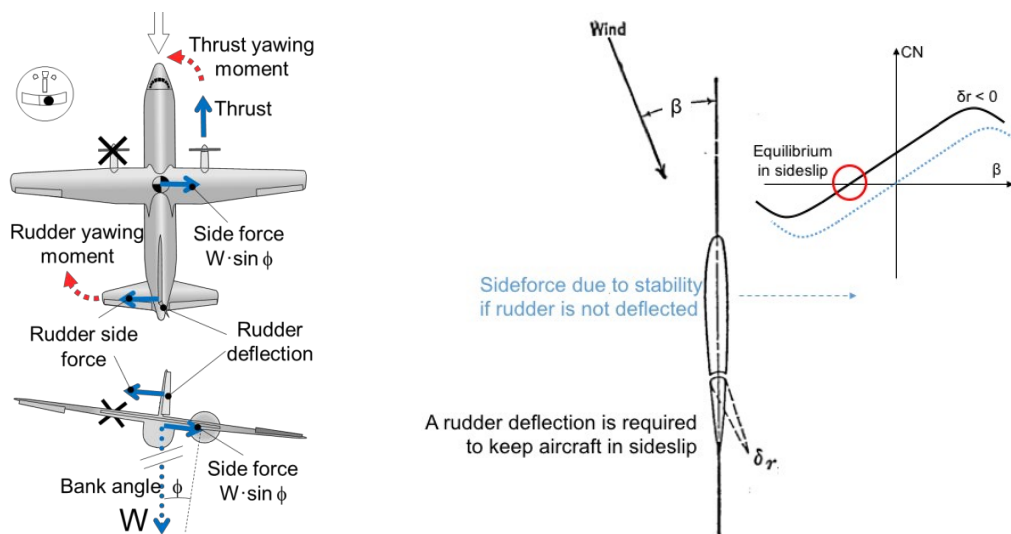


Figure 1: Aircraft directional control in action with one engine inoperative (left, ©Harry Horlings / Wikimedia Commons / CC-BY-SA 3.0) and rudder deflection to keep a given sideslip angle (right).

Another condition not critical for safety, but important for flight quality, is the ratio between directional and lateral static stability derivatives, which should be less than unit for transport aircraft, to avoid the annoying *dutch roll* phenomenon. For general aviation and military aircraft this requirement may be different, especially for the carrier-based airplanes, where large lateral control in landing is vital.

Design of the vertical tail is not a simple task, due to the asymmetrical flow behind the wing-fuselage combination and lateral cross-control (side force on vertical tailplane that causes a rolling moment). These aerodynamic issues must be addressed in both the linear and non-linear range of the lift curve, and aerodynamic interference must be accounted for. Some indications come from aircraft design books [2]-[8]: the first approach is to look at similar aircraft and apply the same tail volume coefficient. This is a non-dimensional number defined as the ratio of vertical tail planform area  $S_v$ , times the longitudinal distance between wing and vertical tail aerodynamic centers  $l_v$ , to the product of wing planform area  $S$  and wing span  $b$

$$\bar{V}_v = \frac{S_v l_v}{S b} \quad (1)$$

The idea is that similar airplanes will have similar stability characteristics. The result gives the designer a first approximation of the vertical tail size to apply in aircraft preliminary design.

In practice, preliminary sizing is based on semi-empirical methods, such as USAF DATCOM [9] or ESDU [10], which calculate the static stability and control derivatives,  $C_{N_\beta}$  and  $C_{N_{\delta_r}}$  respectively, including the effects of the aerodynamic interference. However, these methods are not very accurate because they are based on wind tunnel data obtained in the first half of the XX century on aircraft geometries quite different from actual transport airplanes [11]-[16]. For this reason, the authors developed a new method named VeDSC (Vertical tail Design, Stability, and Control), which is the synthesis of hundreds of numerical RANS (Reynolds-averaged Navier-Stokes) simulations involving many different regional turboprop transport aircraft configurations and validated through wind tunnel tests [16]. These methods are briefly described in the next section.

The aircraft directional stability and control are represented by the values of the derivatives  $C_{N_\beta}$  and  $C_{N_{\delta_r}}$  evaluated in the linear range. Both terms contribute to the aircraft yawing moment coefficient, (non-dimensioned on free-stream dynamic pressure and wing area)

$$C_N = C_{N_\beta}\beta + C_{N_{\delta_r}}\delta_r \quad (2)$$

where the main contributions to the stability derivative are due to the vertical tail and the fuselage

$$C_{N_\beta} = C_{N_{\beta_v}} + C_{N_{\beta_f}} + C_{N_{\beta_w}} \quad (3)$$

assuming that each term includes the mutual aerodynamic interference. The effect of the wing is directly relevant only for moderate to high sweep angle, whereas both wing and horizontal tail have a significant *indirect* effect due to the aerodynamic interference on the vertical tail.

The rudder control derivative  $C_{N_{\delta_r}}$  mainly depends on the rudder effectiveness  $\tau$  and vertical tail planform, along with aerodynamic interference due to the fuselage and horizontal stabilizer. Aerodynamics of aircraft directional control is actually object of a deep investigation by the authors. Next sections will address each term as described by DATCOM, ESDU, and VeDSC methods. The limits of each approach will be clearly highlighted and examples on flying airplanes will be given. Last section concludes the paper with a discussion about critical issues in vertical tail design.

## 2 Directional stability derivative $C_{N_\beta}$

As previously stated, the main contributions to aircraft directional stability derivative  $C_{N_\beta}$  are due to the vertical tail and the fuselage. Historically, all the contributions to aerodynamic interference have been assigned to the vertical tail, whereas the fuselage behavior in sideslip has been considered unaffected [12], [16]. The effects of fuselage, wing, and horizontal tail on the vertical tail have been resumed by USAF DATCOM [9]:

- the fuselage in sideslip conditions exhibits a flow characteristic similar to a cylinder in airflow, where the peak local velocity occurs at the top at the cylinder and it decays to the free stream *cross-flow* value at distance from the body surface. This phenomenon tends to increase the effectiveness of the vertical tail: the fuselage directly alters the vertical tail incidence because of the cross-flow around the body. Hoerner [3] has given another physical explanation: the fuselage acts as an *end-plate* on the vertical tail, being similar to a combination of a wing with a tip tank. Both theories neglect the effect of the vertical tail on the fuselage. The investigation performed by the authors also highlighted that the vertical tail reduces the fuselage instability in sideslip, especially in the non-linear range of the lift curve, as shown in Section 4;
- the vortex system developed by the wing-fuselage combination in sideslip, named *sidewash* and analogous to the downwash in the longitudinal plane, indirectly affects the incidence of the vertical tail. This effect is such to increase the vertical tail contribution to directional

stability if the wing is low with respect to the fuselage; the contrary happens on a high wing-body combination;

- the effect of the horizontal stabilizer on the vertical tail is a change in the pressure loading of the latter, if the former is located at a relatively high or low position. Test data highlight the greater effectiveness of vertical stabilizer in these configurations, a phenomenon named *end-plate effect*. Conversely, a reduction of vertical tail contribution to directional stability is observed if the empennage assumes a cruciform shape.

## 2.1 Vertical tail directional stability derivative $C_{N\beta_v}$

All the methods start from the definition of the vertical tail lift curve slope, which is function of vertical tail planform (aspect ratio and sweep angle), airfoil section, and Mach number

$$C_{L\alpha_v} = \frac{2\pi A_v}{2 + \sqrt{\frac{B^2}{\kappa^2 A_v} \left(1 + \frac{\tan^2 \Lambda_{v,c}/2}{B^2}\right) + 4}} \quad (\text{rad}^{-1}) \quad (4)$$

The definition of vertical tail aspect ratio  $A_v$  changes among the methods, as well as the corrective factors to account for aerodynamic interference. The expression of the lift curve slope depends on the desired approximation: B is a compressibility factor function of the Mach number, whereas  $\kappa$  accounts for the section lift curve slope. See Refs. [7] and [17] for details.

### 2.1.1 USAF DATCOM

The USAF DATA Compendium [9] defines the vertical tail yawing moment coefficient for low angles of attack as

$$C_{N\beta_v} = k_v C_{L\alpha_v} \left[ \eta_v \left(1 - \frac{d\sigma}{d\beta}\right) \right] \frac{l_v}{b} \frac{S_v}{S} \quad (5)$$

where:

$k_v$  is an empirical factor;

$C_{L\alpha_v}$  is function of an effective aspect ratio  $A_{v,\text{eff}}$  due to the fuselage, horizontal tail position and size;

$\eta_v \left(1 - \frac{d\sigma}{d\beta}\right)$  is the sidewash effect;

$\frac{l_v}{b} \frac{S_v}{S}$  is the tail volume coefficient.

In particular, the effective aspect ratio is defined as

$$A_{v,\text{eff}} = \frac{A_v(f)}{A_v} A_v \left[ 1 + k_h \left( \frac{A_v(hf)}{A_v(f)} - 1 \right) \right] \quad (6)$$

where  $A_v = b_v^2/S_v$  is the geometric aspect ratio (see Figure 2) and the ratios in the previous equation are nonlinear functions of vertical tail span to fuselage height in the region of vertical tail,  $b_v/2r$ , and horizontal tail position with respect to vertical tail span,  $z_h/b_v$ , see Figure 3. Some remarks:

- the vertical tail span  $b_v$  is the same of the isolated vertical tail planform;
- when computing the correction factors the vertical tail is extended to the fuselage centerline, together with its span (here named  $b_{v1}$ ) and taper ratio;
- the above mentioned region of the vertical tail is the projection of the quarter point of vertical tail mean aerodynamic chord (m.a.c.) on the fuselage centerline;
- the vertical tailplane m.a.c. is that of the isolated tailplane.

Other details are given in Refs. [7], [9], and [17].

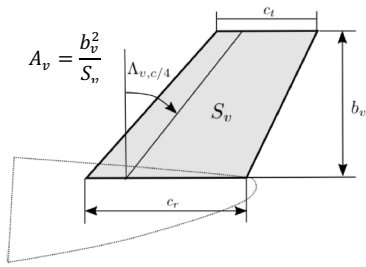


Figure 2: Vertical tail planform definition.

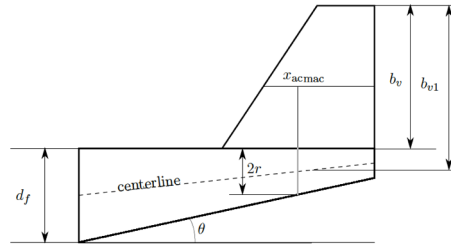


Figure 3: USAF DATCOM definitions.

### 2.1.2 ESDU

The Engineering Science Data Unit provides the following method [10]. The vertical tail aspect ratio is defined as

$$A_F = 2 \frac{b_F^2}{S_F} \quad (7)$$

which is substituted in Eq. 4 in locus of the aspect ratio  $A_v$ . The geometric definitions are reported in Figure 4. The lift curve slope of the isolated vertical tailplane is corrected by three empirical factors,  $J_B$ ,  $J_T$ ,  $J_W$  respectively body-vertical tail, horizontal tailplane, and wing correction factors, and it is scaled by the tail volume coefficient

$$C_{N_{\beta_v}} = J_B J_T J_W C_{L_{\alpha_F}} \frac{l_F S_F}{b S} \quad (8)$$

This method assumes conventional geometries, an almost circular fuselage, and a constant sidewash. It is a synthesis of experimental analyses performed by NACA, British Aerospace, SAAB, and other companies, coupled with potential flow theory where the data were highly scattered. The vertical tail is considered a trapezoidal panel, any extension like dorsal fairing or a curved fin tip is ignored and the leading edge is extended linearly in the body. The tip chord is the chordwise distance between the leading and trailing edges of the fin at the maximum height. The root chord is the chordwise distance between the (extrapolated) leading and trailing edges of the fin at the height where the fin quarter-chord sweep line intersects the top of the body, as shown in Figure 4. Note that the vertical tail planform may be different from that calculated with the DATCOM method.

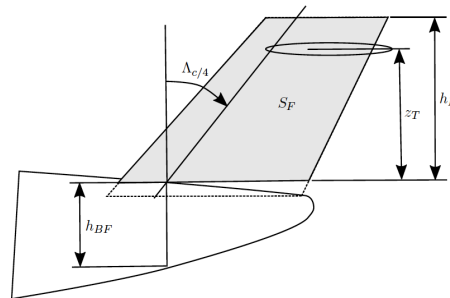


Figure 4: ESDU vertical tail planform definition.

### 2.1.3 USAF DATCOM vs ESDU: application to a regional turboprop

It has been previously stated that semi-empirical methods are inadequate for some configurations. The following example applied on the ATR-42 aircraft (Figure 5) shows that, while both methods give close result for the initial configuration (see Table 1), a parametric investigation reveals that significant differences arise in other conventional aircraft layouts, for instance by changing the wing

position or the horizontal tail position, as shown in Figure 6. In a preliminary design phase, it is unknown which method is best suited for an accurate estimation of the directional stability derivatives.



Figure 5: ATR-42 aircraft.

Derivative (rad <sup>-1</sup> )	$C_{N_{\beta_v}}$
DATCOM	0.276
ESDU	0.273
$\Delta\%$ from DATCOM	-1.09

Table 1: Results of semi-empirical methods on the ATR-42.

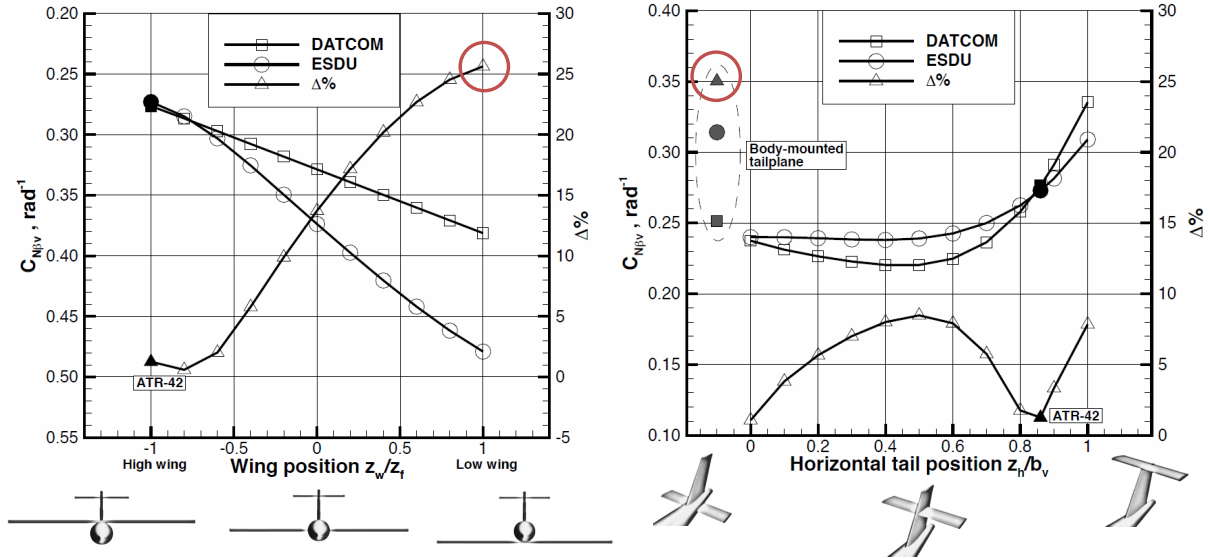


Figure 6: Parametric investigation to compare semi-empirical methods.

#### 2.1.4 VeDSC

The Vertical tail Design, Stability, and Control method has been recently developed by the authors, with the aim to provide a reliable preliminary design method for regional turboprop airplanes. The formulation is similar to that of the ESDU method

$$C_{N_{\beta_v}} = K_{F_v} K_{W_v} K_{H_v} C_{L_{\alpha_v}} \frac{l_v S_v}{b S} \quad (9)$$

where the correction factors have been calculated from the ratio of  $C_{N_{\beta_v}}$  between different configurations, through CFD RANS simulations:

- $K_{F_v}$  is the aerodynamic interference factor of the fuselage on the vertical tail;
- $K_{W_v}$  is the aerodynamic interference factor of the wing on the vertical tail;
- $K_{H_v}$  is the aerodynamic interference factor of the horizontal tail on the vertical tail;
- $C_{L_{\alpha_v}}$  is calculated with Eq. 4;
- $\frac{l_v S_v}{b S}$  is the vertical tail volume coefficient.

The interference factor due to the fuselage is defined as the ratio of the vertical tail stability derivative of the fuselage-vertical tail combination (FV) to the isolated vertical tail (V). Similarly, the interference factor due to the wing is given by the same ratio calculated for the wing-fuselage-tail

combination (WV) against the fuselage-vertical tail configuration (FV). Finally, the effect of the horizontal tail is evaluated by the ratio of vertical tail stability derivative of the complete aircraft (WVH) against the wing-fuselage-vertical tail combination (WV). In mathematical expressions

$$K_{F_v} = \frac{C_{N\beta_v}^{(FV)}}{C_{N\beta_v}^{(V)}} \quad K_{W_v} = \frac{C_{N\beta_v}^{(WV)}}{C_{N\beta_v}^{(FV)}} \quad K_{H_v} = \frac{C_{N\beta_v}^{(WVH)}}{C_{N\beta_v}^{(WV)}} \quad (10)$$

The method accounts for variation of vertical tail planform, fuselage after-body shape, wing position and aspect ratio, horizontal tail position and size, see Figure 7. Results have been resumed in charts where it is clearly represented the variation of the aerodynamic interference factors with the aircraft geometrical parameters. By adding components to a given combination, the number of possible layout configurations increases. For this reason, there is 1 chart representing the effect of the fuselage, 3 charts that describe the effect of the wing, and 9 charts for the effect of the horizontal tail. Only some of them are shown in Figure 8, also because the same number of charts is available for the calculation of the aerodynamic interference on the fuselage. As matter of fact, the nature of the CFD simulations has permitted to easily separate the effects and calculate the contribution to directional stability of each aircraft component. See Ref. [16] for details.

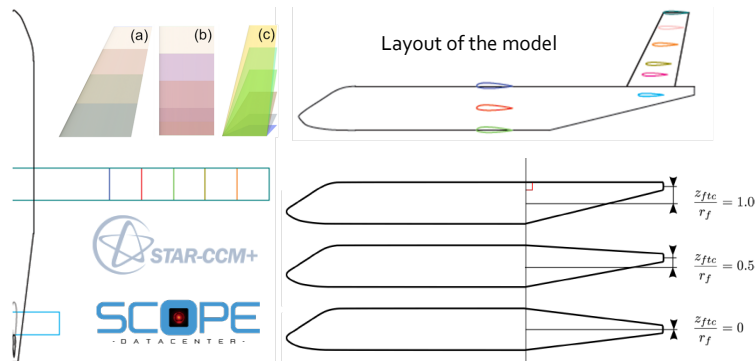


Figure 7: Layout of the aircraft modular model used to develop the VeDSC method.

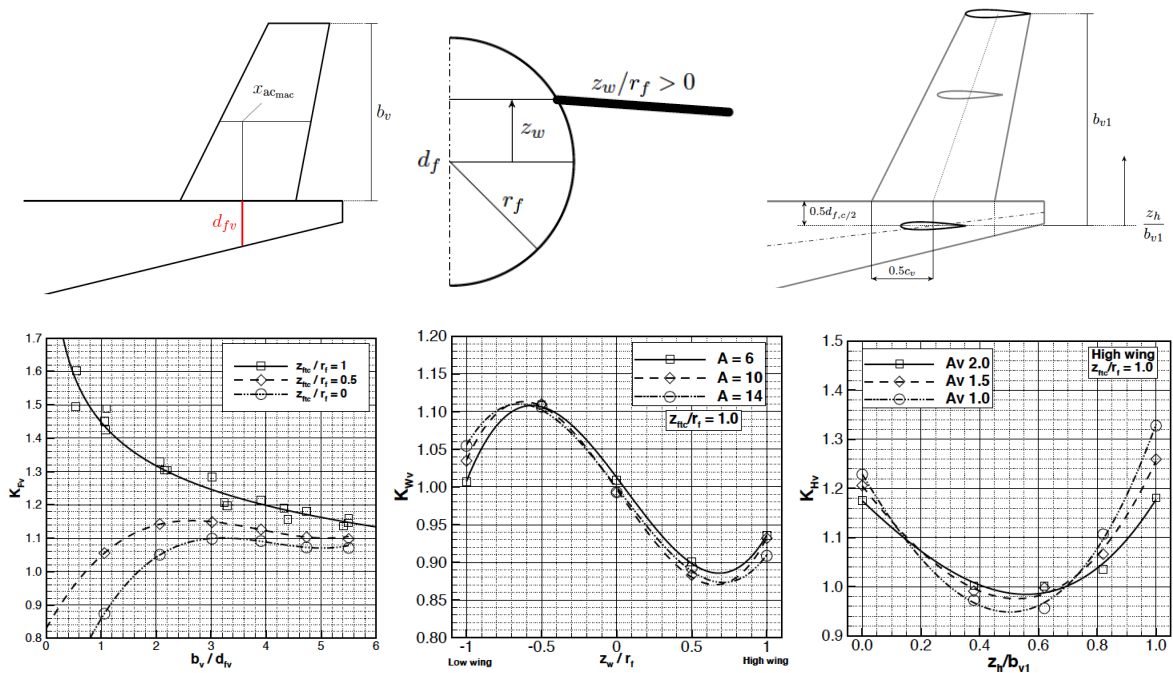


Figure 8: Effects of the fuselage (left), wing (middle), and horizontal tail (right) on the vertical tail.

## 2.2 Fuselage directional stability derivative $C_{N_{\beta f}}$

The semi-empirical methods available to estimate the fuselage contribution to aircraft directional stability  $C_{N_{\beta f}}$  do not account for aerodynamic interference: it is unaffected by the aircraft layout, it depends only on the fuselage shape. Multhopp [18], Perkins [5], and Roskam [7] provided linear semi-empirical formulations that are basically function of the fuselage slenderness ratio (length over maximum diameter). Since the designer, as well as the pilot, is interested in the total aircraft directional stability, it makes sense to assign all the aerodynamic interference effects on the vertical tail and consider the fuselage unaffected: wind tunnel test data usually provide results about the global forces and moments. However, CFD simulations and recent wind tunnel tests performed by the authors have shown that this approach may lead to unsatisfactory results, especially at high angles of sideslip, as reported in Figure 9, which shows a reduction in fuselage  $C_{N_{\beta f}}$  with vertical tail span, and Figure 10, which shows non-linear effects at high sideslip angles. The authors of this paper also developed a method to estimate the aerodynamics of the isolated fuselage [19], whereas the VeDSC method provides aerodynamic interference factors in sideslip due to the vertical tail, wing, and horizontal tail [16]. Further details can be found in the above mentioned references. A correction for high angles of sideslips for isolated fuselage is the following

$$C_{N_f} = K_f \cdot C_{N_{\beta}} \quad (11)$$

$$K_f = \left( \frac{C_{N_f}}{C_{N_{\beta}}} \right)_{\text{Poly}} = 0.2362 + 1.0178 \cdot \beta - 0.0135 \cdot \beta^2$$

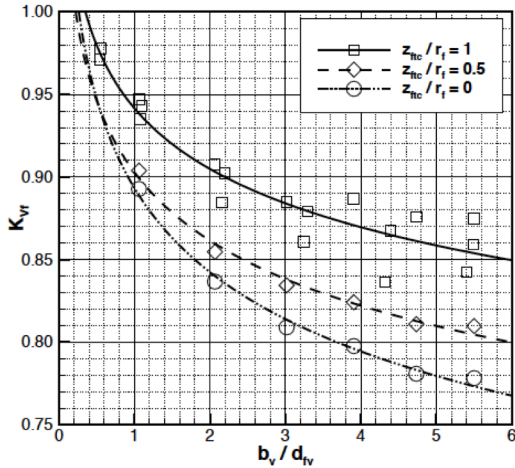


Figure 9: Effects of the vertical tail on the fuselage.

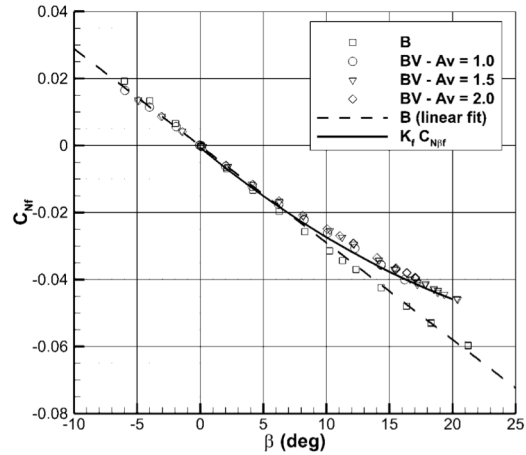
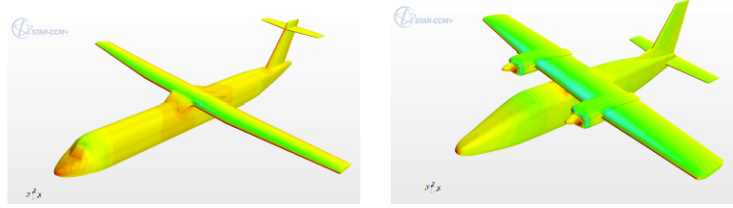


Figure 10: Non-linear effects on the fuselage.

## 2.3 Comparison of the methods on two different aircraft categories

In this section, DATCOM, ESDU, and VeDSC methods are compared on two aircraft representative of the regional turboprop transport (named GRT) and of the commuter layout (Tecnam P2012), shown in Figure 11. It is here remarked that the models investigated are different from that used to develop the VeDSC method. Results are reported in Table 2, where it is apparent the reliability of the new VeDSC method on the regional turboprop transport aircraft class. The relative error ( $\Delta\%$ ) is calculated from the results of CFD analyses, which are in good agreement with wind tunnel test data described in Section 4.



(A) Generic Regional Turboprop. (B) Tecnam P2012.  
Figure 11: Model airplanes used to compare semi-empirical methods.

	Vertical tail		Fuselage			Vertical tail		Fuselage	
	$C_{N_{\beta v}}$ (/deg)	$\Delta\%$	$C_{N_{\beta f}}$ (/deg)	$\Delta\%$		$C_{N_{\beta v}}$ (/deg)	$\Delta\%$	$C_{N_{\beta f}}$ (/deg)	$\Delta\%$
CFD	0.00426	—	-0.00218	—	CFD	0.00274	—	0.00090	—
DATCOM	0.00475	11.5	0.00216	-0.65	DATCOM	0.00187	-31.8	0.00120	33.0
ESDU	0.00490	15.0	—	—	ESDU	0.00273	1.1	—	—
<b>VEDSC</b>	0.00421	-1.09	0.00215	-1.29	<b>VEDSC</b>	0.00255	-7.31	0.00092	2.20

Table 2: Comparison of the results of semi-empirical methods for the GRT (left) and the P2012 (right).

### 3 Directional control derivative $C_{N_{\delta_r}}$

The rudder is the aerodynamic control surface of the vertical tailplane. A preliminary numerical study [13], performed on the same model described in this work, has investigated the effects of aerodynamic interference among aircraft components at several sideslip and rudder deflection angles. Numerical analyses have shown that the deflection of the rudder generates a *local* angle of sideslip on the fuselage after-body. This effect is increased by the fuselage and the horizontal tail, in contrast with the approach of semi-empirical procedures, which evaluate the interference effects as the whole aircraft were in sideslip. The most important parameters that characterize the aerodynamics of directional control (neglecting propeller and flap effects) in cruise conditions are: the vertical tail aspect ratio, the ratio between the vertical tail span and the fuselage diameter at vertical tail aerodynamic center, and the horizontal tailplane position. The wing has a negligible effect, because of its distance from the asymmetric flow field induced by the rudder.

The above mentioned effect is shown in Figure 12, where the fuselage, wing, and horizontal tail are added to the vertical tail, at several angles of sideslip and rudder deflection. In absence of sideslip with  $10^\circ$  of rudder deflection, there is an increase in the sideforce generated by the vertical tail in the presence of the other components with respect to the vertical tail alone. This is attributed to the aerodynamic interference among the aircraft components, which is conserved at angles of sideslip. The solid lines, starting from the origin of the axes, represent the complete and partial aircraft configurations in sideslip, with no rudder deflection ( $\delta_r = 0^\circ$ ). Adding the fuselage, wing, and horizontal tailplane increases the curve slope of the vertical tail sideforce coefficient. The dashed lines represent the same configurations with a rudder deflection of  $\delta_r = 10^\circ$ . In other words, the symbols of the dashed lines on the left edge of the chart are not overlapped as in the case without rudder deflection. Also, it can be observed that the addition of the aircraft components changes the slope and translates the curves, except for the wing contribution, which is negligible. With good approximation, the sideforce generated by the vertical tail has a linear trend. Linearity is particularly important for rudders, because strong non-linearity may cause unacceptable variations in control surfaces.

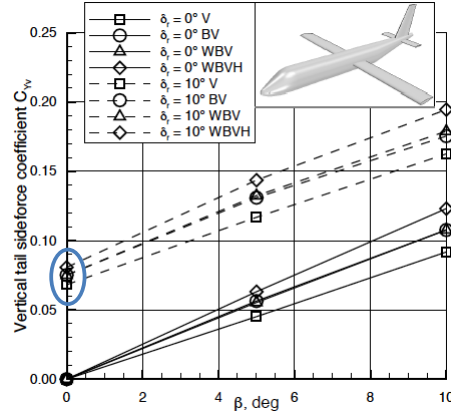


Figure 12: Effects of rudder deflections on vertical tail sideforce in several configurations in sideslip.

The semi-empirical formulation reported by Roskam [7] is essentially the following

$$C_{N_{\delta_r}} = f \left[ C_{L_{\alpha_v}}(A_{veff}), \tau, K_{span} \right] \quad (12)$$

where the lift curve slope of the vertical tail is corrected by  $A_{veff}$ , which is the same calculated with Eq. 6, as the whole aircraft were in sideslip. This is conceptually incorrect, because of the above mentioned local sideslip flow due to the rudder deflection.

A preliminary formulation of the VeDSC method is the following

$$C_{N_{\delta_r}} = C_{L_{\alpha_v}} K_{\delta_r} \tau \frac{S_v l_v}{S b} \quad (13)$$

where  $C_{L_{\alpha_v}}$  is calculated from Eq. 4 with the geometric aspect ratio  $A_v$ , and  $K_{\delta_r}$  is defined as

$$K_{\delta_r} = \begin{cases} 1.07 \left( 1 + \frac{K_{F_v} - 1}{2.2} \right) & \text{for body-mounted tail} \\ (1.33 - 0.09A_v) \left( 1 + \frac{K_{F_v} - 1}{2.2} \right) & \text{for T-tail configuration} \end{cases} \quad (14)$$

while the rudder effectiveness  $\tau$  is object of investigation by the authors. Results on a generic twin-engine commuter aircraft are shown in Figure 13, where it is apparent that semi-empirical methods underestimate the value of the rudder effectiveness at high deflection angles, while CFD and wind tunnel data provide higher results. The high values of the rudder effectiveness are due to the large values of the vertical tail chord ratios: 0.52 at root and 0.73 at tip (shielded horn balance). Similar trends, although with lower values, have been obtained for regional turboprop airplanes.

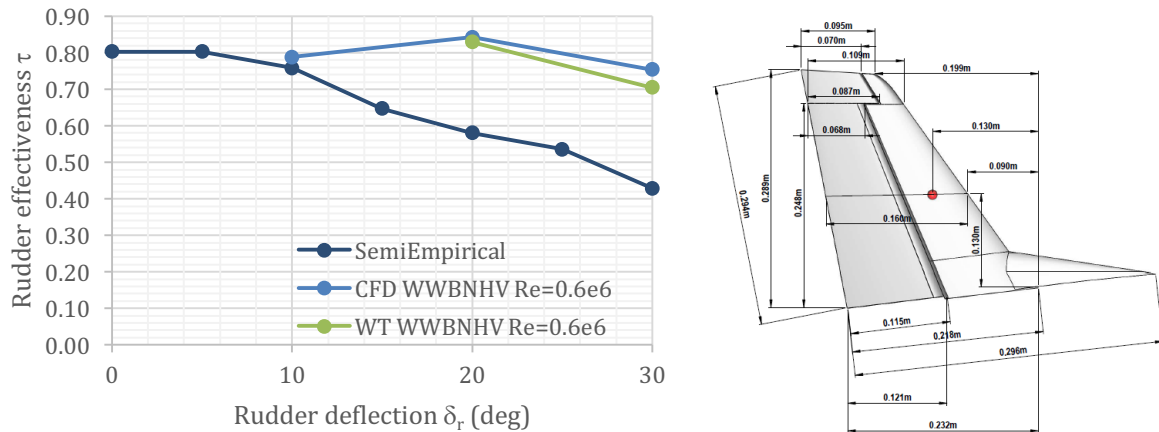


Figure 13: Comparison of rudder effectiveness calculated by semi-empirical methods, CFD simulations, and wind tunnel data on a generic commuter aircraft.

## 4 Wind tunnel testing

The CFD analyses have been validated in the main subsonic wind tunnel of the Dept. of Industrial Engineering of the University of Naples “Federico II”. Full details of the wind tunnel facility and of the tests have been reported in Ref. [16]. Here, for the sake of brevity, few data are shown. The same modular aircraft model of the numerical analyses has been realized (Figure 14). A load cell has been installed in the fuselage tail-cone to directly measure the sideforce generated by the vertical tail, while the strain-gage wind tunnel balance measures the total aerodynamic forces and moments (sideforce, yawing and rolling moments), as shown in Figure 15.

Results about a complete aircraft configuration are shown in Figure 16 on the whole range of the sideslip curve, where a strong agreement between numerical and experimental data is apparent. In Figure 17, wind tunnel tests also show the true repartition of aerodynamic forces on a body-tail configuration with different vertical tail planforms: the fuselage curve slope  $C_{N\beta_f}$  changes in presence of the vertical tail and a further reduction of its instability is observed at high sideslip angles.

The VeDSC method has also been verified during wind tunnel tests. The effects of the horizontal tail position on the vertical tail, for a given tail-cone shape and wing position, are shown in Figure 18. The same philosophy of CFD analyses and wind tunnel testing will be followed for the investigation about rudder effectiveness and aircraft directional control.

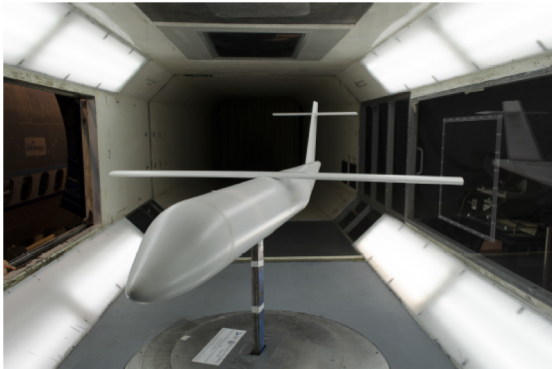


Figure 14: The aircraft model in the wind tunnel.

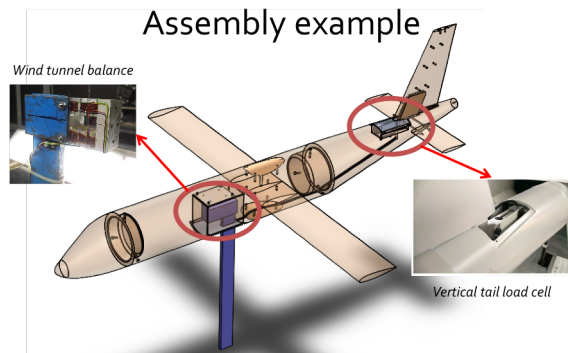


Figure 15: Balance and load cell locations.

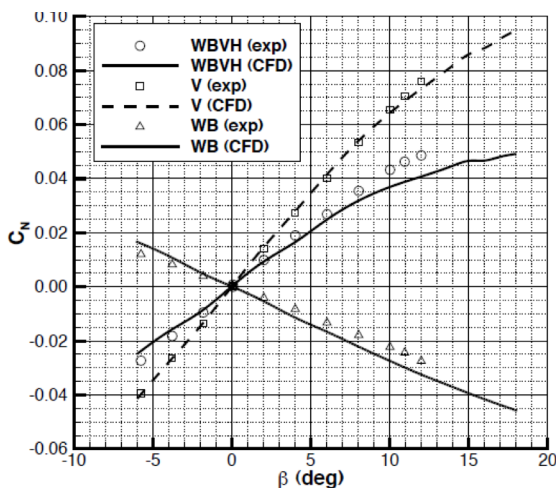


Figure 16: Comparison between CFD and wind tunnel data.

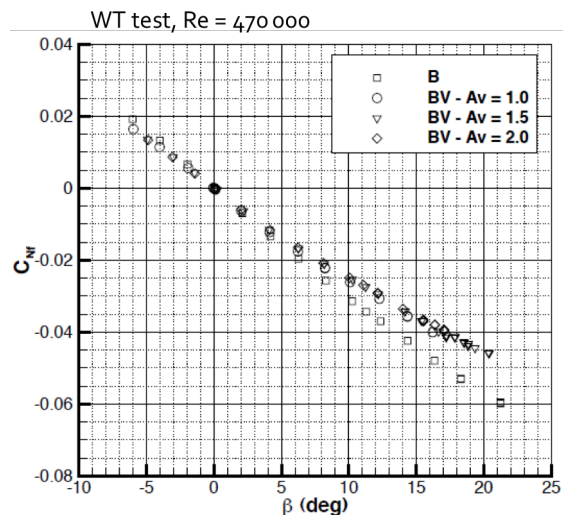


Figure 17: Aerodynamic interference of the vertical tail on the fuselage.

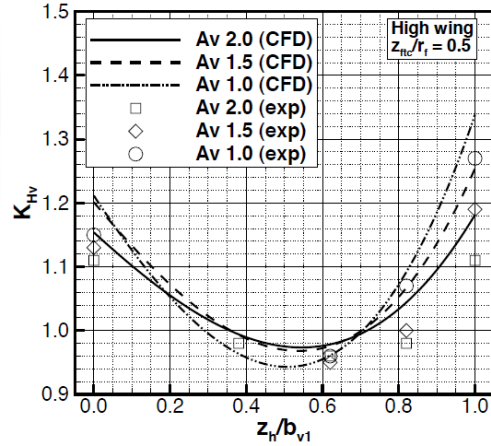
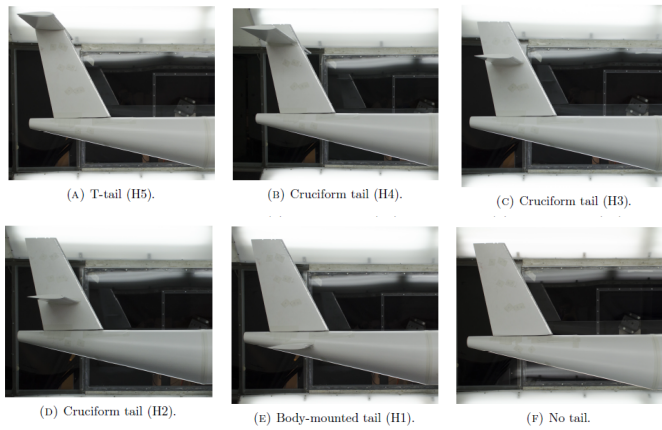


Figure 18: The VeDSC method has also been verified in the wind tunnel.

## 5 Conclusion

This work has described the requirements of vertical tail design and the limits of the available classical semi-empirical methods. Directional stability and control are both crucial times in aircraft safety, performance, and flight qualities. The authors are working with numerical and experimental tests to provide more reliable preliminary design methods for transport aircraft, especially on the regional turbopropeller category. The VeDSC method developed by the authors seems promising in comply with the objective and it will be further extended with data about rudder effectiveness.

To further clarify the importance of stability and control derivatives and the role of the designer, consider the following example. The first condition to size the vertical tail of a multi-engine aircraft like a regional turboprop is the minimum control speed, which must be not higher than 1.13 the takeoff stall speed. Assuming a linear variation of the turboprop engine thrust with airspeed, the chart in Figure 19 shows that for the GRT aircraft (previously analyzed in the comparison of semi-empirical methods) a vertical tail planform area  $S_v = 13 \text{ m}^2$  is sufficient to comply with aviation regulations. However, the aircraft must also be able to cope with high angles of sideslip, say for instance  $\beta > 20^\circ$ . Because of non-linear effects, a larger vertical tail, say  $S_v = 20 \text{ m}^2$ , may not be able to trim the aircraft at the required sideslip angle, as shown in Figure 20. Such tail is also heavier, provides more parasite drag, and does not add any advantage in airborne minimum control speed, since the aircraft cannot fly below the stall speed (the intersection between the engine curve and the tail curve with  $S_v = 20 \text{ m}^2$  in Figure 19 is at about 0.97 take-off stall speed). For this reason, the ratio  $C_{N\beta}/C_{N\delta_r} = d\delta_r/d\beta$  should be slightly less than unit. In fact, the maximum yawing moment coefficients generated by both sideslip angle and rudder deflection must be comparable, as shown by the solid lines in Figure 21, otherwise the higher value obtained in  $C_N$  with the larger vertical tail area can trim sideslip angles only up to  $13^\circ$ , as shown by the dashed lines in Figure 21. In this example, the rudder effectiveness  $\tau$  has been calculated with semi-empirical methods and it is shown in Figure 22.

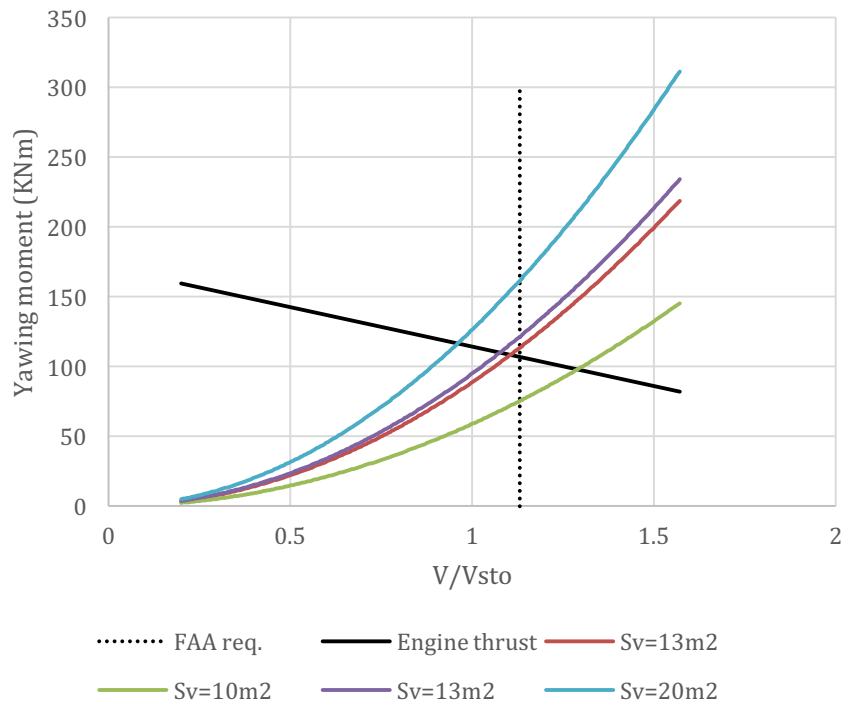


Figure 19: Vertical tail area required to cope with airborne minimum control speed.

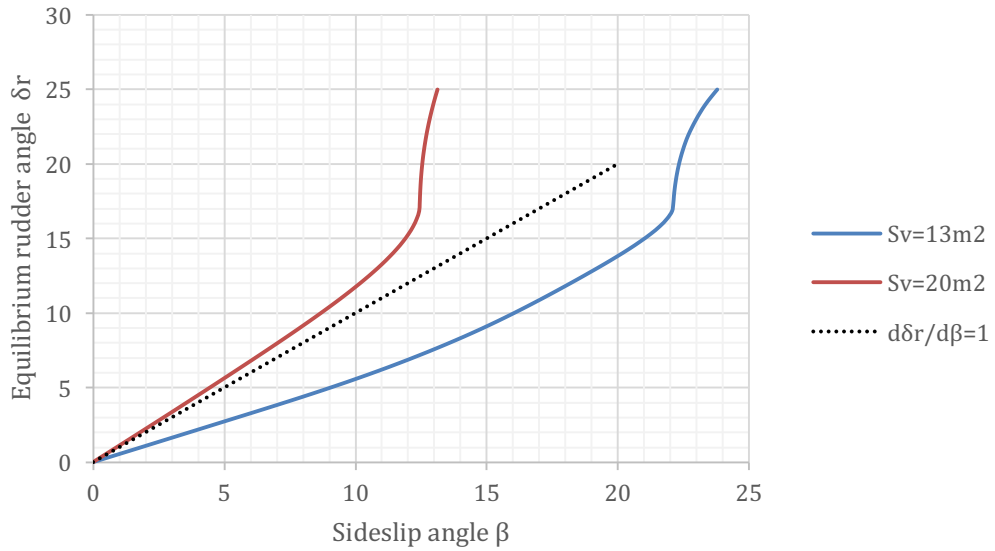


Figure 20: Rudder angle required to keep a given sideslip angle.

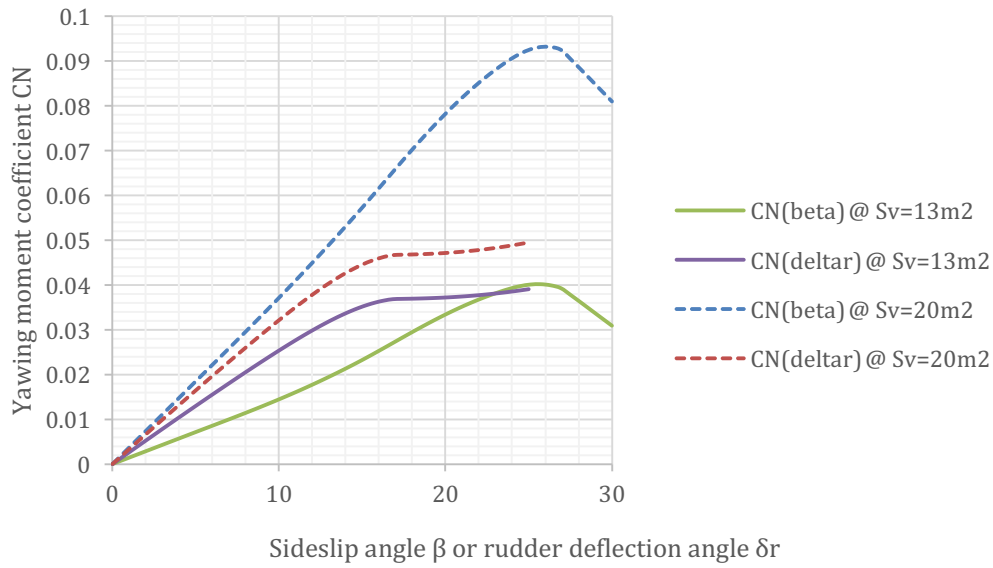


Figure 21: Yawing moment coefficients obtainable with sideslip and rudder deflection.

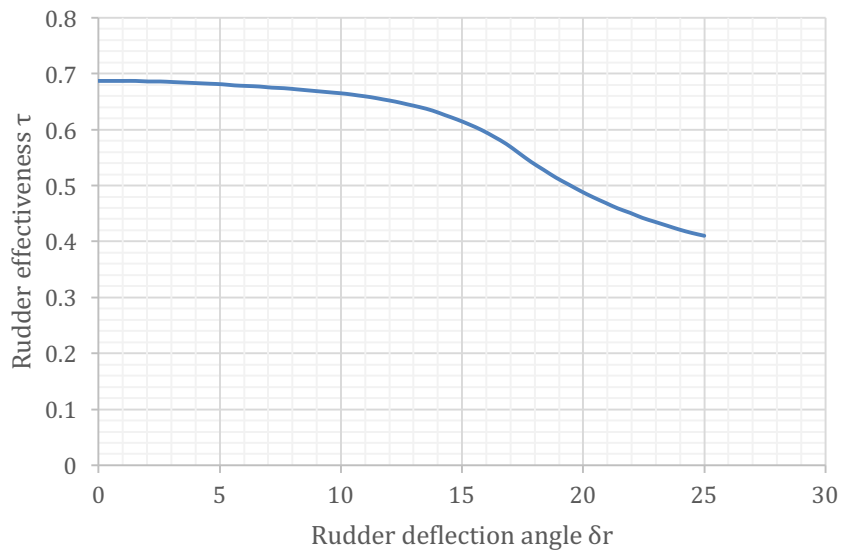


Figure 22: Rudder effectiveness variation with rudder deflection.

In conclusion, to properly design a vertical tail it is fundamental to accurately estimate the directional stability derivatives  $C_{N\beta}$  and  $C_{N\delta_r}$ . As previously shown, non-linearity is important too. These can be resumed in: vertical tail and fuselage yawing moment coefficients  $C_N$  at high angles of sideslip  $\beta$  (mutual aerodynamic interference effects) and rudder effectiveness  $\tau$  at high rudder deflection angles  $\delta_r$  (at both low and high sideslip angles  $\beta$ ).

## References

- [1] EASA: Acceptable Means of Compliance for Large Aeroplanes CS-25. Tech. Rep. Amendment 17. European Aviation Safety Agency, 2015.
- [2] Gudmundsson, S.: General aviation aircraft design: applied methods and procedures. Butterworth-Heinemann, 2013, ISBN 9780123973290.
- [3] Hoerner, S. F.: Fluid-Dynamic Lift. Published by the author, 1985, ISBN 9789998831636.
- [4] Obert E. Aerodynamic design of transport aircraft. Ios Press, Amsterdam, The Netherlands, 2009. ISBN 9781586039707.
- [5] Perkins, C. D., Hage, R. E.: Airplane performance stability and control. Wiley, New York, 1949, ISBN 9780471680468.
- [6] Raymer, D. P.: Aircraft design: a conceptual approach. AIAA education series. American Institute of Aeronautics and Astronautics, Reston, VA, 5th edition, 2012. ISBN 9781600869112.
- [7] Roskam, J.: Airplane design Part VI. DARcorporation, Lawrence (KS), 2000, ISBN 9781884885525.
- [8] Torenbeek, E.: Synthesis of subsonic airplane design. Delft University Press, Delft, 1982. ISBN 9024727243.
- [9] Finck, R. D.: USAF stability and control DATCOM. AFWAL-TR-83-3048, McDonnell Douglas Corporation, Wright-Patterson Air Force Base, Ohio, 1978.
- [10] Gilbey, R. W.: Contribution of fin to sideforce, yawing moment and rolling moment derivatives due to sideslip,  $(Y_v)_F$ ,  $(N_v)_F$ ,  $(L_v)_F$ , in the presence of body, wing and tailplane. Item 82010, ESDU, 1982.
- [11] Ciliberti, D., Nicolosi, F., Della Vecchia, P.: A new approach in aircraft vertical tailplane design. In: 22th AIDAA Conference, Associazione Italiana di Aeronautica e Astronautica, 2013.
- [12] Nicolosi, F., Della Vecchia, P., Ciliberti, D.: An investigation on vertical tailplane contribution to aircraft sideforce. In: Aerospace Science and Technology 28.1 (2013), pp. 401–416.
- [13] Nicolosi, F., Della Vecchia, P., Ciliberti, D.: Aerodynamic interference issues in aircraft directional control. In: Journal of Aerospace Engineering, 2014.
- [14] Nicolosi, F. et al.: Development of new preliminary design methodologies for regional turboprop aircraft by CFD analyses. In: ICAS 2014 Proceedings, International Council of the Aeronautical Sciences, Optimage Ltd., 2014.
- [15] Della Vecchia, P., Nicolosi, F., Ciliberti, D.: Aircraft directional stability prediction method by CFD. In: 33rd AIAA Applied Aerodynamics Conference, 2015.
- [16] Ciliberti, D.: An improved preliminary design methodology for aircraft directional stability prediction and vertical tailplane sizing. PhD Thesis, YouCanPrint, 2016, ISBN 9788892608825.
- [17] Chappell, P. D., Gilbey, R. W.: Lift-curve slope and aerodynamic centre position of wings in inviscid subsonic flow. ESDU Item 70011. Engineering Science Data Unit, 1970.
- [18] Multhopp, H.: Aerodynamics of the Fuselage. NACA Technical Memorandum 1036. National Advisory Committee for Aeronautics, 1942.
- [19] Nicolosi, F. et al.: Fuselage aerodynamic prediction methods. In: Aerospace Science and Technology 55 (2016), pp. 332–343.